Available online at www.sciencedirect.com
ScienceDirect
Atmospheric Environment 40 (2006) 7882–7892
ATMOSPHERIC ENVIRONMENT
www.elsevier.com/locate/atmosenv

Formation and growth of indoor air aerosol particles as a result of D-limonene oxidation

E. Vartiainen[a,b,*], M. Kulmala[a], T.M. Ruuskanen[a], R. Taipale[a], J. Rinne[a], H. Vehkamäki[a]

[a]*Department of Physical Sciences, University of Helsinki, P.O. Box 64, FIN-00014 Helsinki, Finland*
[b]*Finnish Institute of Occupational Health, Topeliuksenkatu 41 a A, FIN-00250 Helsinki, Finland*

Received 10 March 2006; received in revised form 14 July 2006; accepted 17 July 2006

Abstract

Oxidation of D-limonene, which is a common monoterpene, can lead to new aerosol particle formation in indoor environments. Thus, products containing D-limonene, such as citrus fruits, air refresheners, household cleaning agents, and waxes, can act as indoor air aerosol particle sources. We released D-limonene into the room air by peeling oranges and measured the concentration of aerosol particles of three different size ranges. In addition, we measured the concentration of D-limonene, the oxidant, and the concentration of ozone, the oxidizing gas. Based on the measurements we calculated the growth rate of the small aerosol particles, which were 3–10 nm in diameter, to be about 6300 nm h^{-1}, and the losses of the aerosol particles that were due to the coagulation and condensation processes. From these, we further approximated the concentration of the condensable vapour and its source rate and then calculated the formation rate of the small aerosol particles. For the final result, we calculated the nucleation rate and the maximum number of molecules in a critical cluster. The nucleation rate was in the order of 10^5 cm^{-3} s^{-1} and the number of molecules in a critical-sized cluster became 1.2. The results were in agreement with the activation theory.

Keywords: Nucleation; Particle growth; Activation; Monoterpene oxidation; Indoor air particle sources

1. Introduction

In the absence of aerosol particle sources the aerosol particle concentration indoors typically follows the pattern of outdoor concentration (Raunemaa et al., 1989; Koponen et al., 2001; Hussein et al., 2004). In addition, various indoor activities such as cooking, dusting, vacuum cleaning, or heating can increase the aerosol particle number and mass concentration indoors (He et al., 2004; Hussein et al., 2005, 2006). The indoor aerosol particles thus come from primary as well as secondary sources with varying source strengths. The strongest reported number-based indoor air aerosol particle sources include cooking, especially frying or grilling, smoking, heating, and burning candles (He et al., 2004; Afshari et al., 2005).

The gas and the particle phase reactions of the terpenes and the oxidants such as ozone in an

*Corresponding author. Finnish Institute of Occupational Health, Topeliuksenkatu 41 a A, FIN-00250 Helsinki, Finland. Tel.: +358 40 042 7698.
E-mail address: eija.vartiainen@helsinki.fi (E. Vartiainen).

1352-2310/$ - see front matter © 2006 Elsevier Ltd. All rights reserved.
doi:10.1016/j.atmosenv.2006.07.022

indoor environment can result in high aerosol particle concentrations as shown by e.g. Wainman et al. (2000) and Weschler and Shields (1999). The D-limonene is a monoterpene which is commonly present in indoor air (Brown et al., 1994). In addition to citrus fruits, products such as air fresheners, waxes, and cleaning agents often contain D-limonene (Liu et al., 2004; Nazaroff and Weschler, 2004; Wainman et al., 2000). Hoffmann et al. (1997) reported the high mass-based aerosol yield of D-limonene indoors in the presence of oxidants. In addition, chamber studies conducted by Rohr et al. (2003) indicate a significant increase in ultrafine aerosol particle number concentrations as a result of D-limonene oxidation. Also Nøjgaard et al. (2006) reported the high aerosol number concentration during ozonolysis of D-limonene. These aerosol particles are formed through nucleation and condensation processes. Study by Bonn and Moortgat (2002) shows that reactions with ozone have the biggest impact in nucleation of monoterpenes.

The formation of new aerosol particles through homogeneous or heterogeneous nucleation in the atmosphere affects the earth's radiative balance and is thus an important phenomenon. Recent knowledge on the atmospheric nucleation is summarized by Kulmala et al. (2004). The role of the organic vapours in the aerosol particle formation and growth processes under typically prevailing environmental conditions is a key issue. It is suggested that organic species contribute to the growth of nucleated clusters (etc. O'Dowd et al., 2002; Anttila and Kerminen, 2003). Koch et al. (2000) studied aerosol particle formation as a result of the ozonolysis of several monoterpenes in a laboratory experiment. Their results also showed the high aerosol yield of this process. They concluded that in favourable conditions the monoterpene oxidation can have an effect on atmospheric aerosol particle formation. Despite the intensive study of the subject, the mechanism of aerosol particle formation is yet unsolved.

Currently, knowledge of monoterpene oxidation under realistic environmental conditions is incomplete. The ultrafine aerosol particle production ability of monoterpenes in indoor air, the following health impacts, and the mechanism of outdoor aerosol particle production and its atmospheric relevance are of particular interest.

The first motivation for the study was the observation of exceptionally high aerosol particle production after peeling citrus fruits. As citrus plants store large amounts of monoterpenes, mainly limonene, in their peels (see e.g. Högnadóttir and Rouseff, 2003; Moufida and Marzouk, 2003), peeling the fruits releases limonene into the air. In addition to aerosol particle number concentrations we measured the concentration of monoterpenes and ozone. Our aim is to increase knowledge of D-limonene containing products as potential indoor air ultrafine and fine aerosol particle sources as well as to clarify the mechanisms of new aerosol particle formation in natural environments.

2. Calculation method for vapour concentration and nucleation rate

The theory on the formation and growth of the aerosol particles as a result of the condensing and nucleating organic vapours is explained in more detail by Kulmala et al. (2001). Thus, we will only briefly go through the main steps used in our study.

Nucleation rate (Kerminen and Kulmala, 2002)

$$J_1 = J_3 \exp\left[\frac{\eta}{d_{p_1}} - \frac{\eta}{d_{p_3}}\right] \tag{1}$$

is the rate at which the critical-sized clusters of approximately 1 nm vapourize. The J_3 in Eq. (1) is the formation rate of the 3 nm-sized aerosol particles and term η is given by

$$\eta = \frac{\gamma C_S}{2\pi D G_R}. \tag{2}$$

Thus, the η depends on the particle growth rate G_R, diffusion coefficient D, factor γ, and the condensation sink

$$C_S = 4\pi D \sum_i \beta_i r_i N_i. \tag{3}$$

Now, β is the transitional correction factor given by Fuchs and Sutugin (1971) and r_i is the particle radius. Factor γ, which is given by (Kerminen and Kulmala, 2002)

$$\gamma = \gamma_0 \left[\frac{d_{p_1}}{1\,\text{nm}}\right]^{0.2} \left[\frac{d_{p_3}}{3\,\text{nm}}\right]^{0.075} \left[\frac{T}{293\,\text{K}}\right]^{-0.75} \times \left[\frac{\rho}{1000\,\text{kg m}^{-3}}\right]^{-0.33} \left[\frac{d_{\text{mean}}}{150\,\text{nm}}\right]^{0.048}, \tag{4}$$

takes into account environmental conditions such as the initial nuclei size d_{p_1}, the observed particle size d_{p_3}, the temperature T, the nuclei density ρ, and the mean diameter of the pre-existing aerosol particle number size distribution d_{mean}. Factor γ_0 ($= 0.23\,\text{nm}^2\,\text{m}^2\,\text{h}^{-1}$) is a constant.

The formation rate of 3 nm aerosol particles is given by (Kulmala et al., 2001)

$$J_3 = \frac{dN_3}{dt} + K_3 N_3 + \frac{\Delta N_3}{\Delta d_p} G_R. \quad (5)$$

In Eq. (5) dN_3/dt is the change in aerosol particle number concentration of small particles, in the 3–10 nm in diameter size fraction. Furthermore, Δd_p is the width of the size fraction, ΔN_3 is the number of aerosol particles, and K_3 is their coagulation sink

$$K_i = \sum_j K_{ij} N j. \quad (6)$$

The coagulation sink K_3 is the loss of the aerosol particles in size class 3–10 nm, with the approximated mean size of 5 nm, as they coagulate with the pre-existing, over 10 nm-sized, aerosol particles and with each other. The coagulation sink for the aerosol particles in size class i depends on the aerosol particle number concentration N_i in this size class as well as on the coagulation coefficient K_{ij} between the aerosol particles in class i with the pre-existing aerosol particles in class j.

We can calculate the aerosol particle growth rate (Kulmala, 1988),

$$\frac{dr}{dt} = \frac{m_v \beta_m D C}{r \rho}, \quad (7)$$

by comparing the measured number concentrations of 3 and 10 nm diameter aerosol particles. The growth rate depends on vapour concentration C as well as on diffusion coefficient D and molecular mass m_v. We used a value of 0.06 $cm^2 s^{-1}$ for the vapour diffusion coefficient and a value of 180 amu for the molecular mass. As we know the aerosol particle growth rate we can thus calculate the vapour concentration by integrating from Eq. (7). We chose the value of 180 amu for the molecular mass of the condensing vapour as it is close to the molecular masses of many known reaction products such as limononaldehyde or limonic acid. Also, we will later notice that the results are only slightly dependent on the molecular mass. In contrast, the value of the diffusion coefficient can have a substantial effect on the results. We based our calculation of the diffusion coefficient on the method presented by Fuller (see e.g. Poling et al., 2001). Because we were unable to ascertain what condensable vapour was present, we calculated the diffusion coefficient for limononaldehyde, limonic acid, and limononic acid. The resulting diffusion coefficients were of the same order of magnitude, around 0.06 $cm^2 s^{-1}$.

The D-limonene is consumed in reactions with the ozone and the OH radical. Concentration of the condensable vapour as a function of time (Kulmala, 1988)

$$\frac{dC}{dt} = Q - C_S C, \quad (8)$$

depends on the vapour source rate Q as well as on the condensation sink. Thus, if we know the vapour source rate we may calculate the vapour concentration as a function of time and further get the growth rate from Eq. (7).

According to the kinetic theory, the nucleation rate depends on the square of the concentration of the condensing vapour (Laakso et al., 2004),

$$J_1 = k_{kin} C^2, \quad (9)$$

where the pre-factor k_{kin} remains constant in a stable environment. However, in some cases the exponent in the nucleation rate is even smaller than two (see Kulmala et al., 2006). In this case the existing clusters are activating and the nucleation rate is

$$J_1 = k_{act} C, \quad (10)$$

where the activation coefficient k_{act} is proportional to the fraction of clusters to be activated per second.

3. Measurements and instrumentation

We conducted the measurements in a laboratory room in prevailing room temperature and ventilation circumstances. We peeled two oranges, the second orange 136 s after the first one, to release D-limonene into the room air. We measured aerosol particle concentrations, concentration of monoterpenes and ozone during the peeling process and continued the measurements for a few hours. We measured the monoterpene concentration with a time resolution of 1.5 s, the ozone concentration with a time resolution of 15 s, and the aerosol particle number concentration with a time resolution of 1 s.

We measured the aerosol particle concentration using TSI condensation particle counter (CPC) models 3025, 3022, and 3010. The three CPC models had slightly different cut-off sizes: 3, 7 and 10 nm, respectively. Thus, we were able to determine concentrations of aerosol particles in three size groups: 3–7, 7–10 nm, and larger than 10 nm. There

was an exceptionally high background concentration of aerosol particles and thus we diluted the air let to the CPCs by a factor of $\frac{1}{3.5}$.

Monoterpene concentration was determined with a proton transfer reaction–mass spectrometer (PTR–MS, Ionicon GmbH, Innsbruck, Austria). The instrument uses a soft ionization method in which volatile organic compounds (VOCs) with a proton affinity higher than that of water go through a proton transfer reaction with hydronium ions (Lindinger et al., 1998). Many VOCs can be detected at their molecular mass plus one, while some go through partial fragmentation. To determine the D-limonene concentration we measured the protonated molecular mass of monoterpene of 137 amu as well as the protonated masses of possible monoterpene fragments of 81, 82, and 95 amu reported by Tani et al. (2003). We determined that with our measurement set-up of the PTR-MS the concentration of mass 137 corresponded to 49% of the total monoterpene concentration. The monoterpene emissions from orange peel can be assumed to consist mainly of D-limonene (Steinbrecher et al., 1999; Orav and Kann, 2001; Högnadóttir and Rouseff, 2003; Moufida and Marzouk, 2003). Thus, we assumed that D-limonene concentration equals the monoterpene concentration. In addition, we measured the ozone concentration using an ultraviolet light absorption analyser (Model 49, Thermo Environmental Instruments, Franklin, MA, USA).

4. Results and discussion

Peeling of oranges indoors, where enough oxidant is present, results in a high concentration of small, ultrafine aerosol particles. At first we detected this in the indoor air size distribution measurements (Vartiainen et al., 2004) where we observed a significant increase in the aerosol particle number concentration after the peeling of an orange (Fig. 1). In those measurements a differential mobility particle sizer (DMPS) measured the aerosol particle number size distributions. Nucleation was not observed in simultaneously measured outdoor aerosol particle number size distribution (Fig. 2). The first two indoor aerosol particle bursts appeared as a result of the orange peeling. As seen from Fig. 1, the aerosol particles emerged in the smallest size class where the aerosol particle diameter is around 3 nm following which the aerosol particles quickly grew towards bigger sizes. The total aerosol particle number concentration increased tenfold after the orange peeling and the growth rate was several hundred nanometers per hour, which was too high to be accurately deduced from the DMPS data.

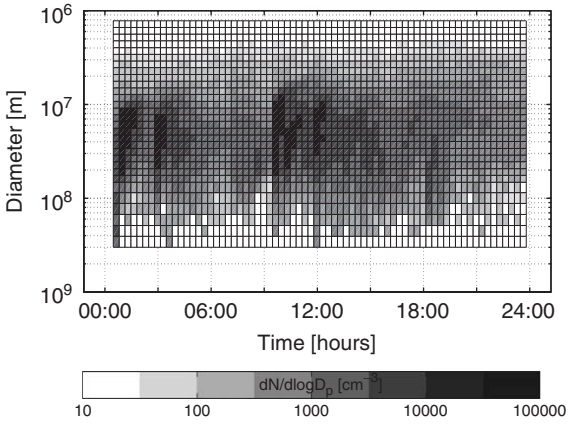

Fig. 1. Measured indoor air particle size distribution on 29th of September 2003. Dark colour indicates a high number concentration of aerosol particles whereas the lighter colour corresponds to a lower number concentration of aerosol particles. Rapid growth of the aerosol particles formed in peeling an orange process is very noticeable.

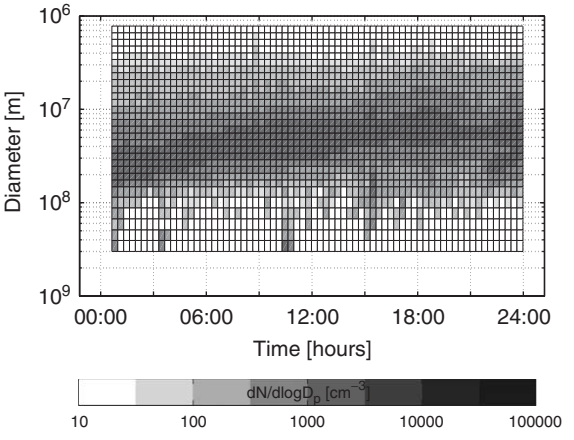

Fig. 2. Measured outdoor air particle size distribution on 21st of September 2003. The distribution is measured simultaneously with the indoor air particle size distribution shown in Fig. 1. Dark colour indicates a high number concentration of aerosol particles whereas the lighter colour corresponds to a lower number concentration of aerosol particles.

The time resolution of the DMPS measurement was inadequate for more detailed information on aerosol particle formation and growth processes. Thus, we conducted a new measurement with three CPCs with substantially better time resolution

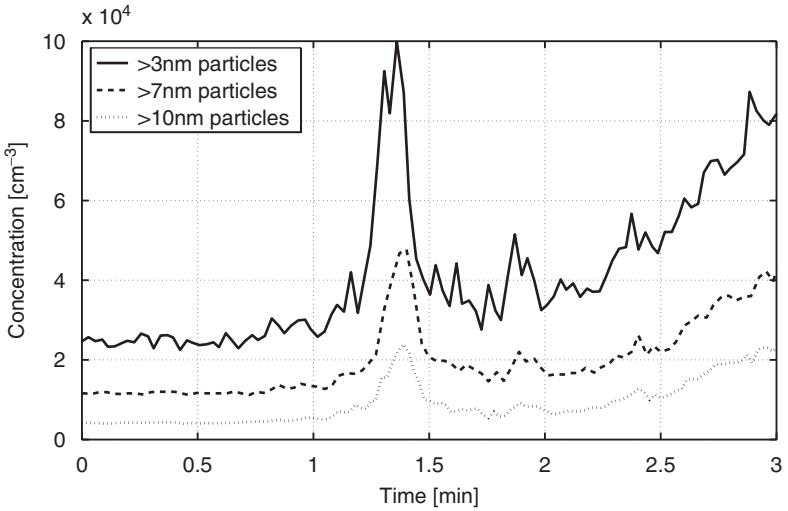

Fig. 3. Diluted concentrations of the aerosol particles over 3, 7, and 10 nm in diameter as measured by different CPC models in the laboratory experiment. The *x*-axis shows the time which begins from the moment when we peeled the first orange.

(Fig. 3) and monitored the oxidation of D-limonene with ozone (Fig. 4). In this experiment we observed the formation of new aerosol particles due to gas and particle phase reactions. Despite the dilution of the aerosol particle measurements sample, only CPC model 3022 was able to measure the highest observed concentrations of aerosol particles.

5. Yield and growth rate of aerosol particles

The concentration of D-limonene increased for the first 400 s and the concentration of ozone simultaneously decreased (Fig. 4). A rapid increase in the aerosol particle number concentration appeared 70 s after the first orange peeling. The formed aerosol particles disappeared quickly due to rapid growth and coagulation. The number concentration started to increase again after the first aerosol particle burst but the growth was slower compared to the growth during the first concentration peak.

We calculated the growth rate of the aerosol particles based on the measured time difference between the peak concentrations of the 3 nm (CPC 3025) and the 10 nm (CPC 3010) aerosol particles. The time difference, according to Fig. 3, is about 4 s which gives a particle growth rate of 6300 nm h^{-1}.

The observed growth rate is very high, especially if we compare it to the typical growth rates observed in ambient atmospheric conditions (Kulmala et al., 2004). Because we had quite a high background

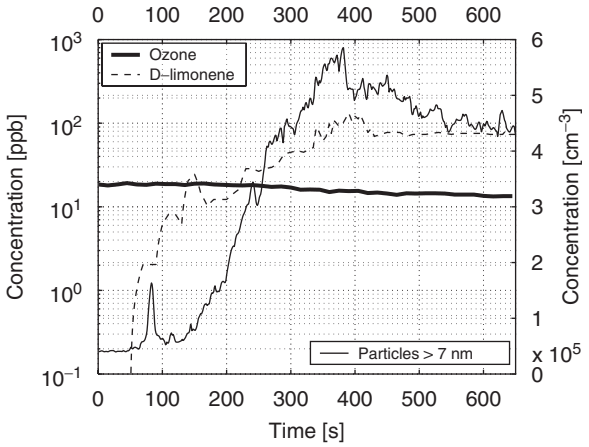

Fig. 4. Concentration of D-limonene and ozone and number concentration of over 7 nm diameter aerosol particles as a function of time after peeling an orange at the time 0 s.

concentration of aerosol particles the growth rate could be partly explained by intramodal coagulation. Thus, we calculated, according to the formulas presented by Stolzenburg et al. (2005), the effect of the background aerosol on the observed growth rates. Depending on the modal structure of the background aerosol, which we had to guess because of lack of data, the contribution of the intra- and extramodal coagulation to the total growth rate was not more than 1%. Thus, we concluded that the growth was mainly condensational in which coagulation played only a minor role.

6. Losses of aerosol particles and vapour molecules during growth

With CPC model 3025 we were able to detect the newly formed aerosol particles only after they had reached the measurable size of 3 nm. Before the aerosol particles grew to this size a part of them coagulated with the pre-existing aerosol particles. We took coagulation into account in the aerosol particle formation rate calculations. The coagulation sinks for 1, 2, and 3 nm aerosol particles, which we calculated according to Eq. (6), are presented in Fig. 5. In the calculations we assumed that the background concentration of the aerosol particles was equal to the sum of the concentrations of two aerosol particle classes with diameters above 10 nm and between 3 and 10 nm. In the calculation of the coagulation coefficients we assumed that the mean diameters for these two aerosol particle size classes were 50 and 5 nm. In this case, as the growth rate of the aerosol particles was high, the effect of the coagulation was small. This meant that the formation rate of the 3 nm-sized aerosol particles was very close to the nucleation rate. The condensation sink, which is also presented in Fig. 5, removes the vapour molecules and thus decreases the amount of condensable vapour. The condensation sink depends on the amount of pre-existing aerosol particles according to Eq. (3).

7. Concentration of condensable vapour and vapour source rate

As the first approximation we assumed a steady-state situation where the concentration of the condensable vapour was constant. Concentration of condensable vapour is linked to particle growth rate according to Eq. (7). With the observed growth rate of 6300 nm h^{-1}, the vapour diffusion coefficient of 0.06 cm^2 s^{-1}, and the molecular mass of 180 amu, the concentration of the condensable vapour becomes 4.3×10^{10} cm^{-3}. As the vapour concentration was assumed constant we were able to further calculate the time-dependent vapour source rate from Eq. (8). At 80 s, when the growth rate was calculated, the vapour source rate was 1.3×10^{9} cm^{-3} s^{-1}.

Ozone molecules react with D-limonene molecules to form primary and secondary reaction products. Some of the reaction products which have low vapour pressures may nucleate or condense onto the particle surfaces. If ozone is the primary oxidant of the D-limonene, ozone molecules should disappear at approximately the same rate as the reaction products are formed in the D-limonene–ozone reaction. The reaction constant for the D-limonene–ozone reaction according to Hoffmann et al. (1997) is 200×10^{-18} cm^3 $molecule^{-1}$ s^{-1}. Fig. 6 presents the cumulative ozone loss and the cumulative reaction product yield. After about 10 min the amount of the consumed ozone was indeed close

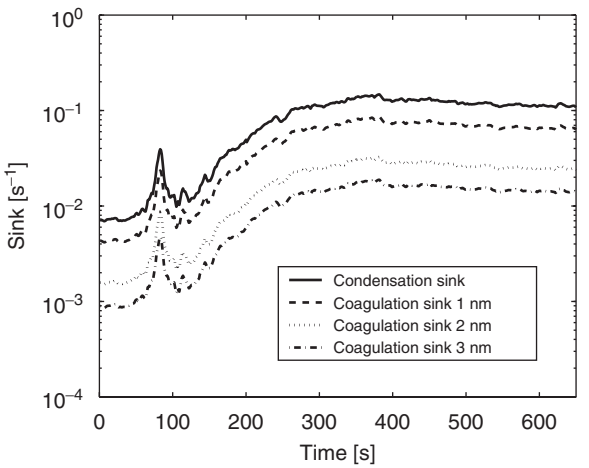

Fig. 5. Condensation and coagulation sinks for 1, 2, and 3 nm diameter aerosol particles. The time in the *x*-axis begins from the moment when we peeled the first orange.

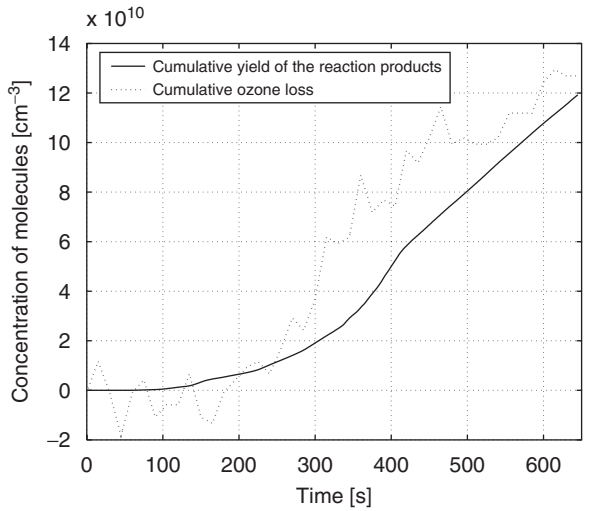

Fig. 6. Cumulative ozone loss and cumulative production of reaction products in reactions of D-limonene with ozone at the time 0 s we peeled the first orange.

to the amount of the reaction products formed. Thus, it appeared that almost all the ozone was consumed in the reactions with the D-limonene molecules.

In addition, D-limonene can react with the OH radical. As the reaction constant of D-limonene with OH is $171 \times 10^{-12}\,\mathrm{cm^3 molecule^{-1} s^{-1}}$ (Hoffmann et al., 1997), D-limonene reacts faster with the hydroxyl radical than ozone. According to the study by Weschler and Shields (1997), where the concentration of OH was measured in a realistic-type indoor environment, the concentration of hydroxyl was approximately $7 \times 10^5\,\mathrm{molecules\,cm^{-3}}$. This is lower than typical outdoor daytime concentration. The concentration of hydroxyl indoors can, however, be even lower, depending on alkene and ozone concentrations (Weschler and Shields, 1996). For example, the model results show that with an ozone concentration of 20 ppb and D-limonene concentration of 2.9 ppb (which is close to the concentrations in this study), the resulting hydroxyl concentration is 4.2×10^{-6} ppb (Weschler and Shields, 1996). The main sources of indoor hydroxyl radicals are outdoor air and reactions of ozone with alkenes. Reactions of D-limonene molecules with ozone thus produce OH. Nevertheless, the reaction also acts as an OH sink. Thus, OH concentration is not very sensitive to D-limonene concentration (Weschler and Shields, 1996). Here, we assumed that the OH radical indoor concentration was relatively low and remained constant and thus it did not affect the calculations or the results.

The steady-state assumption is only a rough estimation of the real behaviour of the concentration of the condensable vapour. If we assumed that the vapour source rate depends linearly on the limonene and the ozone concentrations,

$$Q(t) = \mathrm{Coef} \cdot C_{\mathrm{lim}}(t) \cdot O_3(t), \tag{11}$$

we would get a coefficient with which we could calculate the vapour source rate, and furthermore, the vapour concentration, according to Eq. (8), as a function of time. We calculated the coefficient Coef using the source rate value calculated at the same time as the growth rate. Fig. 7 shows the vapour source rate as a function of time, as calculated using both the linear approximation method presented above as well as the steady-state assumption. In Fig. 8 we present the concentration of the condensable vapour in steady-state and non-steady-state situations.

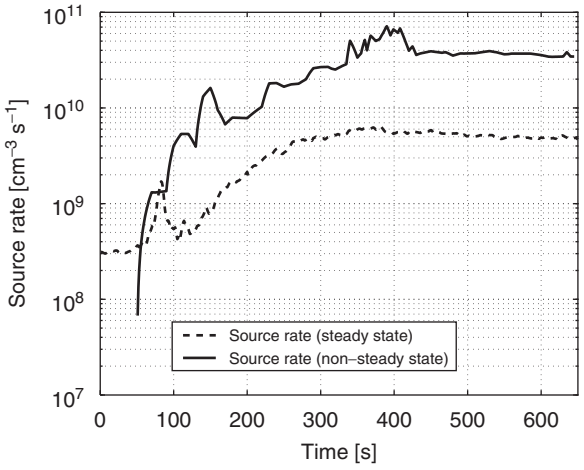

Fig. 7. Vapour source rate for a steady-state vapour concentration case and for a case where the concentration depends linearly on the D-limonene and ozone concentration. The x-axis shows the time in seconds from the peeling of the first orange.

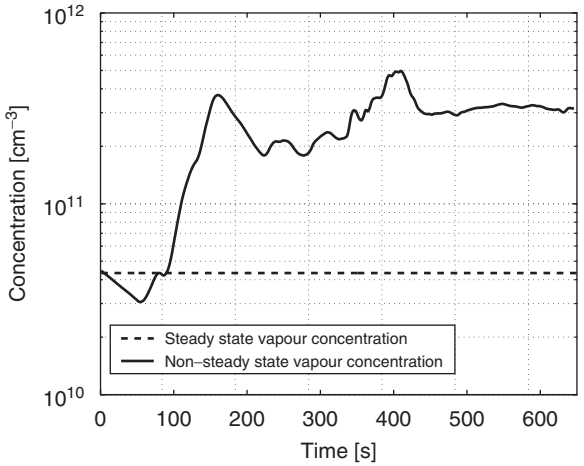

Fig. 8. Calculated concentration of condensable vapour. The concentration is calculated with a steady-state assumption and by assuming a linear dependence of the measured D-limonene concentration. Time on the x-axis begins from the moment when we peeled the first orange.

8. Rate and mechanism of new aerosol particle formation

Nucleation rate here means the formation rate of the 1 nm-sized aerosol particles (J_1). We calculated the nucleation rate based on the measured formation rate of the 3 nm aerosol particles (J_3) according to Eq. (1). In the calculation of the factor γ in Eq. (4), we used the mean diameter of the

background aerosol which corresponded to the mean of the two modes with approximated mean diameters of 5 and 50 nm. The formation rate of the 3 nm aerosol particles was calculated from Eq. (5).

The nucleation rate followed the increase of D-limonene concentration (Fig. 9). The logarithmic slope of the nucleation rate as a function of the concentration of condensable vapours is proportional to the amount of molecules in formed critical clusters (Fig. 10). In fact, using the nucleation theorem (see e.g. Kulmala et al., 2006), the slope gives us the number of molecules in the critical cluster. Now the slope was 1.3 for formation of 3 nm aerosol particles and 1.2 for 1 nm aerosol particles. These results, as well as the fact that the slope was smaller for 1 than 3 nm aerosol particles, are in agreement with the activation theory. We also determined the activation coefficient (k_{act}) from Eq. (10) and it was around 10^{-7}–$10^{-6}\,s^{-1}$ (Table 1) which is in agreement with the results obtained by Kulmala et al. (2006). In contrast, the value of the kinetic pre-factor (k_{kin}) according to Eq. (9) was around 10^{-18}–$10^{-16}\,cm^{-3}s^{-1}$ (Table 1) which is too small to refer to kinetic nucleation. This showed that new aerosol particle formation was mainly due to the activation of existing thermodynamically stable clusters.

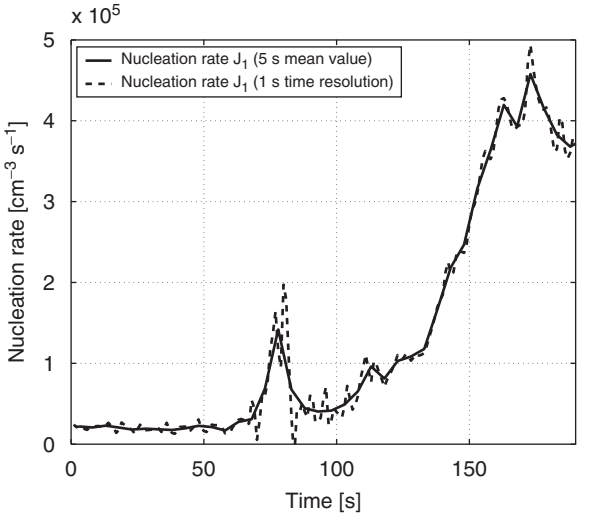

Fig. 9. Nucleation rate as a function of time. The thicker line is the 5 s average of the determined 1 s nucleation rate. The *x*-axis presents the time in seconds from the peeling of the first orange.

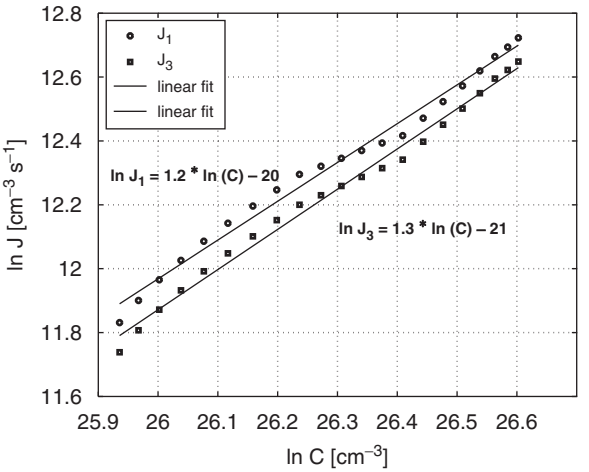

Fig. 10. The logarithm of the nucleation rate and the 3 nm particle formation rate as a function of the logarithm of the concentration of the condensable vapours calculated from 135 to 155 s when the change in the nucleation rate and in the vapour concentration was relatively stable.

9. Sensitivity analysis

We varied the input values of the molecular mass, the aerosol particle density, the accommodation coefficient, the aerosol particle growth rate, and the diffusion coefficient in reasonable limits. Even though in reality the value of the molecular mass depends on the value of the diffusion coefficient we ignored this because the effect is presumably small and we did not have information on the actual condensing vapour. Thus, we received an estimate on the contribution of these changes in starting values to the resulting value of the vapour concentration (C), nucleation rate (J_1), and to the kinetic pre-factor (k_{kin}) and the activation coefficient (k_{act}). In addition, we calculated the influence on the values of the logarithmic slopes of the nucleation rate and formation rate of 3 nm-sized aerosol particles as a function of the concentration of condensable vapours. Changes in the values of the molecular mass and the aerosol particle density had only a small effect on the results. The results were more sensitive to the values of the growth rate, the diffusion coefficient, and the accomodation coefficient (Table 1). However, only a significant change in the values of the growth rate and the accomodation coefficient altered the achieved results more consequentially. As we used the growth rate value of $1000\,nm\,h^{-1}$ the value of the activation coefficient became unrealistically small ($1.0 \times 10^{-3}s^{-1}$) and thus we considered that presumption unreasonable.

Some uncertainties also arose due to the fact that we did not know the actual size distribution of the

Table 1
Concentration of the condensable vapour molecules (C), nucleation rate (J_1), value of the kinetic theory pre-factor (k_{kin}), and the activation coefficient (k_{act}) with the varying values of the molecular mass (m_v), particle density (ρ), accommodation coefficient (α), growth rate (G_R), and diffusion coefficient (D) calculated at 80 s after orange peeling

m_v (amu)	ρ (g cm^{-3})	α	G_R (nm h^{-1})	D (cm^2 s^{-1})	$C \times 10^{10}$ (cm^{-3})	$J_1 \times 10^5$ (cm^{-3} s^{-1})	k_{kin} (cm^3 s^{-1})	k_{act} (s^{-1})	$\Delta \ln(J_1)/\Delta \ln(C)$	$\Delta \ln(J_3)/\Delta \ln(C)$
180	1	1	6300	0.06	4.3	2.0	1.0×10^{-16}	4.5×10^{-6}	1.2	1.3
180	1	1	1000	0.06	0.7	71.6	1.5×10^{-13}	1.0×10^{-3}	0.9	1.2
180	1	1	15000	0.06	10.3	2.4	2.2×10^{-17}	2.3×10^{-6}	1.3	1.3
180	1	0.1	6300	0.06	42.3	0.9	5.1×10^{-19}	2.2×10^{-7}	1.5	1.5
180	2	1	6300	0.06	8.7	1.7	2.2×10^{-17}	1.9×10^{-6}	1.2	1.3
136	1	1	6300	0.06	5.7	2.0	6.0×10^{-17}	3.4×10^{-6}	1.2	1.3
180	1	1	6300	0.01	0.26	2.0	2.9×10^{-18}	7.6×10^{-7}	1.3	1.4
180	1	1	6300	0.1	2.6	2.0	2.9×10^{-16}	7.6×10^{-6}	1.2	1.3

We also calculated the values of the slopes, which are connected to the number of molecules in a critical-sized cluster, with different starting values.

aerosol particles but guessed the mean values of the two size classes, 3–10 and >10 nm, to be 5 and 50 nm. Thus, we also examined the results in cases where these mean diameters attained somewhat diverging values. Tests with values 3 and 8 nm for the smaller size class and 20 and 70 nm for the bigger size class gave a bit diverging results but the activation coefficient, the nucleation rate, and the slopes remained in the same order of magnitude (Table 2). Also, changing the presumed cut-off sizes of the CPCs from 3 and 10 nm to 2 and 5 nm and to 8 and 13 nm did not make consequental changes to the final results (Table 2).

10. Conclusions

The D-limonene oxidation is a strong source of indoor air aerosol particles. The total aerosol particle concentration increased nearly tenfold after we released D-limonene into the room by peeling oranges. The amount of D-limonene and ozone in the room was however moderate: concentration of D-limonene was between 0 and 800 ppb and concentration of ozone was between 10 and 20 ppb. Thus, we may conclude that even in relatively clean indoor environments the oxidation of D-limonene is a potential source of small aerosol particles of size below 3 nm.

The aerosol particles are formed as a result of the nucleation of the secondary reaction products. The formed aerosol particles grow rapidly due to condensation and intramodal coagulation. Even though the background aerosol concentration during the experiment was relatively high, the effect of coagulation on growth is small. The intra- and extramodal coagulations explain only 1% or less of the total growth rate, and the high growth rate of the small aerosol particles is explained mainly by condensation.

The calculated concentration of the condensable vapour depends on the growth rate, the density of aerosol particles, the diffusion coefficient, the molecular mass, and the accommodation coefficient. When we used the observed growth rate of 6300 nm h^{-1}, the accommodation coefficient 1, the density 1 g cm^{-3}, and the molecular mass of 180 amu, the concentration of the condensable vapour was 4.3×10^{10} cm^{-3}. The calculated nucleation rate at the time when growth rate was calculated was 2.0×10^5 cm^{-3} s^{-1}. From these we calculated the value for the activation coefficient k_{act} in the activation theory which was

Table 2
Sensitivity analysis of the cut-off sizes of the CPCs and of estimated mean diameters of the two aerosol particle size class to the final result

Dp_{cut_1} (nm)	Dp_{cut_2} (nm)	Dp_{mean_1} (nm)	Dp_{mean_2} (nm)	G_R (nm h^{-1})	$C \times 10^{10}$ (cm^{-3})	$J_1 \times 10^5$(cm^{-3} s^{-1})	k_{kin}(cm^3 s^{-1})	k_{act} (s^{-1})	$\Delta \ln(J_1)/\Delta \ln(C)$	$\Delta \ln(J_3)/\Delta \ln(C)$
3	10	5	50	6300	4.3	2.0	1.0×10^{-16}	4.5×10^{-6}	1.2	1.3
2	10	5	50	7200	5.0	1.5	5.9×10^{-17}	2.9×10^{-6}	1.2	1.3
5	10	5	50	4500	3.1	3.7	3.8×10^{-16}	1.2×10^{-5}	1.2	1.3
3	8	5	50	4500	3.1	2.8	2.9×10^{-16}	8.9×10^{-6}	1.2	1.3
3	13	5	50	9000	6.2	1.5	4.0×10^{-17}	2.5×10^{-6}	1.2	1.3
3	10	3	50	6300	4.3	1.9	1.0×10^{-16}	4.4×10^{-6}	1.2	1.3
3	10	8	50	6300	4.3	2.1	1.1×10^{-16}	4.8×10^{-6}	1.2	1.3
3	10	5	20	6300	4.3	1.0	5.4×10^{-17}	2.3×10^{-6}	1.3	1.4
3	10	5	70	6300	4.3	3.9	2.1×10^{-16}	9.1×10^{-6}	1.2	1.3
3	10	3	20	6300	4.3	1.0	5.3×10^{-17}	2.3×10^{-6}	1.4	1.4
3	10	8	70	6300	4.3	4.2	2.2×10^{-16}	9.7×10^{-6}	1.2	1.3

Dp_{cut_1} here is the cut-off size of the CPC model 3025, Dp_{cut_2} is the cut-off size of the CPC model 3010, Dp_{mean_1} is the estimated mean diameter of the 3–10 nm aerosol particles, Dp_{mean_2} is the estimated mean diameter of the >10 nm aerosol particles, G_R is the aerosol particle growth rate, C is the concentration of the condensable vapour, J_1 is the nucleation rate, k_{kin} is the kinetic pre-factor, and k_{act} is the activation coefficient. $\Delta \ln(J_1)/\Delta \ln(C)$ is the change of logarithmic nucleation rate divided by logarithmic vapour concentration. The slope thus gives an estimate of the number of molecules in a critical-sized cluster. $\Delta \ln(J_3)/\Delta \ln(C)$ is the change of logarithmic formation rate of 3 nm-sized aerosol particles (J_3) divided by logarithmic vapour concentration. Results, except for the slopes, are calculated at 80 s after orange peeling.

4.5×10^{-6} s^{-1} and thus in reasonable limits. The slope of $\Delta \ln(J_1)/\Delta \ln(C)$, which refers to the activation ofthe existing clusters, had a gradient of 1.2. The activation theory seems to describe the aerosol particle formation pretty well.

Sensitivity of the results proved reasonable. As we used slightly different values of the molecular mass, the particle density, the accomodation coefficient, the growth rate, and the diffusion coefficient, the concentration of the condensable vapour varied between 0.26×10^{10} and 42.3×10^{10} cm^{-3} and the nucleation rate varied between 0.9×10^5 and 2.4×10^5 cm^{-3} s^{-1}. The value of the activation coefficient varied between 2.2×10^{-7} and 7.6×10^{-6} s^{-1} and the value of the slope $\Delta \ln(J_1)/\Delta \ln(C)$ is between 1.2 and 1.5. In addition, we tested the effect of changing the cut-off sizes of the CPCs and the mean diameters of the aerosol particle size classes on the results. Even then the results remain in the same order of magnitude and the final result of the nucleation mechanism, connected to the value of the slope $\Delta \ln(J_1)/\Delta \ln(C)$, did not change. From these tests we can conclude that the results are not sensitive to the starting values.

These promising results indicate that primary nucleation mechanism in D-limonene indoor oxidation is activation. Values of the slope $\Delta \ln(J_1)/\Delta \ln(C)$ and also the kinetic pre-factor were too small to fit with kinetic nucleation. However, this is a preliminary study and the results are restricted to concern the type of situations valid in this experiment. It would be important to repeat the measurements in other environments and also add some additional measurements, such as the size distribution and composition of background aerosols, to confirm and generalize the results.

References

Afshari, A., Matson, U., Ekberg, L., 2005. Characterization of indoor sources of fine and ultrafine particles: a study conducted in a full-scale chamber. Indoor Air 15, 141–150.

Anttila, T., Kerminen, V.-M., 2003. Condensational growth of atmospheric nuclei by organic vapours. Journal of Aerosol Science 34, 41–61.

Bonn, B., Moortgat, G., 2002. New particle formation during α- and β-pinene oxidation by O_3, OH and NO_3, and the influence of water vapour: particle size distribution studies. Atmospheric Chemistry and Physics 2, 183–196.

Brown, S., Sim, M., Abramson, M., Gray, C., 1994. Concentrations of volatile organic compounds in indoor air—a review. Indoor Air 4, 123–134.

Fuchs, N., Sutugin, A., 1971. In: Hidy, G., Brock, J. (Eds.), Topics in Current Aerosol Research. Pergamon, New York.

He, C., Morawska, L., Hitchins, J., Gilbert, D., 2004. Contribution from indoor sources to particle number and mass concentrations in residential houses. Atmospheric Environment 38, 3405–3415.

Hoffmann, T., Odum, J.R., Bowman, F., Collins, D., Klockow, D., Flagan, R.C., Seinfeld, J.H., 1997. Formation of organic aerosols from the oxidation of biogenic hydrocarbons. Journal of Atmospheric Chemistry 26, 189–222.

Högnadóttir, A., Rouseff, R.L., 2003. Identification of aroma active compounds in orange essence oil using gas chromatography–olfactometry and gas chromatography–mass spectrometry. Journal of Chromatography A 998, 201–211.

Hussein, T., Hämeri, K., Aalto, P., Asmi, A., Kakko, L., Kulmala, M., 2004. Particle size characterization and the indoor-to-outdoor relationship of atmospheric aerosols in Helsinki. Scandinavian Journal of Work, Environment and Health 30, 54–62.

Hussein, T., Hämeri, K., Heikkinen, M.S., Kulmala, M., 2005. Indoor and outdoor particle size characterization at a family house in Espoo—Finland. Atmospheric Environment 39, 3697–3709.

Hussein, T., Glytsos, T., Ondráček, J., Dohányosová, P., Ždímal, V., Hämeri, K., Lazaridis, M., Smolík, J., Kulmala, M., 2006. Particle size characterization and emission rates during indoor activities in a house. Atmospheric Environment 40, 4285–4307.

Kerminen, V.-M., Kulmala, M., 2002. Analytical formulae connecting the "real" and the "apparent" nucleation rate and the nuclei number concentration for atmospheric nucleation events. Journal of Aerosol Science 33, 609–622.

Koch, S., Winterhalter, R., Uherek, E., Kolloff, A., Neeb, P., Moortgat, G.K., 2000. Formation of new particles in the gas-phase ozonolysis of monoterpenes. Atmospheric Environment 34, 4031–4042.

Koponen, I.K., Asmi, A., Keronen, P., Puhto, K., Kulmala, M., 2001. Indoor air measurement campaign in Helsinki Finland 1999—the effect of outdoor air pollution on indoor air. Atmospheric Environment 35 (8), 1465–1477.

Kulmala, M., 1988. Ph.D. Dissertation, University of Helsinki.

Kulmala, M., Maso, M.D., Mäkelä, J., Pirjola, L., Väkevä, M., Aalto, P., Miikkulainen, P., Hämeri, K., O'Dowd, C., 2001. On the formation, growth and composition of nucleation mode particles. Tellus 53B, 479–490.

Kulmala, M., Vehkamäki, H., Petäjä, T., Maso, M.D., Lauri, A., Kerminen, V.-M., Birmili, W., McMurry, P., 2004. Formation and growth of ultrafine atmospheric particles: a review of observations. Journal of Aerosol Science 35, 143–176.

Kulmala, M., Lehtinen, K., Laaksonen, A., 2006. Cluster activation theory as an explanation of the linear dependence between formation rate of 3 nm particles and sulphuric acid concentration. Atmospheric Chemistry and Physics 6, 787–793.

Laakso, L., Anttila, T., Lehtinen, K.E., Aalto, P., Kulmala, M., Hörrak, U., Paatero, J., Hanke, M., Arnold, F., 2004. Kinetic nucleation and ions in boreal forest particle formation events. Atmospheric Chemistry and Physics 4, 2353–2366.

Lindinger, W., Hansel, A., Jordan, A., 1998. On-line monitoring of volatile organic compounds at pptv levels by means of proton-transfer-reaction mass spectrometry (PTR-MS) medical applications, food control and environmental research. International Journal of Mass Spectrometry and Ion Processes, 191–241.

Liu, X., Mason, M., Krebs, K., Sparks, L., 2004. Full-scale chamber investigation and simulation of air freshener emissions in the presence of ozone. Environmental Science and Technology 38, 2802–2812.

Moufida, S., Marzouk, B., 2003. Biochemical characterization of blood orange, sweet orange, lemon bergamot and bitter orange. Phytochemistry 62, 1283–1289.

Nazaroff, W.W., Weschler, C.J., 2004. Cleaning products and air fresheners: exposure to primary and secondary air pollutants. Atmospheric Environment 38, 2841–2865.

Nøjgaard, J.K., Bilde, M., Stenby, C., Nielsen, O.J., Wolkoff, P., 2006. The effect of nitrogen dioxide on particle formation during ozonolysis of two abundant monoterpenes indoors. Atmospheric Environment 40, 1030–1042.

O'Dowd, C.D., Aalto, P., Hämeri, K., Kulmala, M., Hoffmann, T., 2002. Atmospheric particles from organic vapours. Nature 416, 497.

Orav, A., Kann, J., 2001. Determination of peppermint and orange aroma compounds in food and beverages. Proceedings of the Estonian Academy of Sciences. Chemistry 50, 217–225.

Poling, B.E., Prausnitz, J.M., O'Connell, J.P., 2001. The Properties of Gases and Liquids, fifth ed. McGraw-Hill Professional, New York.

Raunemaa, T., Kulmala, M., Saari, H., Olin, M., Kulmala, M., 1989. Indoor air aerosol model: transport indoors and deposition of fine and coarse particles. Aerosol Science and Technology 11, 11–25.

Rohr, A.C., Weschler, C.J., Koutrakis, P., Spengler, J.D., 2003. Generation and quantification of ultrafine particles through terpene/ozone reaction in a chamber setting. Aerosol Science and Technology 37, 65–78.

Steinbrecher, R., Hauff, K., Rössler, J., Dürr, M., Seufert, G., 1999. Monoterpene emission from soils in orange plantations of the Valencian Citrus Belt, Spain. Physics and Chemistry of the Earth B 24, 695–698.

Stolzenburg, M.R., McMurry, P.H., Sakurai, H., Smith, J.N., Mauldin III, R.L., Eisele, F.L., Clement, C.F., 2005. Growth rates of freshly nucleated atmospheric particles in Atlanta. Journal of Geophysical Research 110, D22S05.

Tani, A., Hayward, S., Hewitt, C., 2003. Measurement of monoterpenes and related compounds by proton transfer reaction-mass spectrometry (PTR-MS). International Journal of Mass Spectrometry, 561–578.

Vartiainen, E., Hämeri, K., Kuuspalo, K., Nevalainen, A., Toivola, M., Vehkamäki, H., 2004. Journal of Aerosol Science II, 739–740 (Abstracts of the EAC 2004).

Wainman, T., Zhang, J., Weschler, C., Lioy, P., 2000. Ozone and limonene in indoor air: a source of submicron particle exposure. Environmental Health Perspectives 108, 1139–1145.

Weschler, C.J., Shields, H.C., 1996. Production of the hydroxyl radical in indoor air. Environmental Science and Technology 30, 3250–3258.

Weschler, C.J., Shields, H.C., 1997. Measurements of the hydroxyl radical in a manipulated but realistic indoor environment. Environmental Science and Technology 31, 3719–3722.

Weschler, C.J., Shields, H.C., 1999. Indoor ozone/terpene reactions as a source of indoor particles. Atmospheric Environment 33, 2301–2312.